Geophys. J. Int. (2000) **140,** 535–542

A resampling approach to test stress-field uniformity from fault data

Dario Albarello

Dip. di Scienze della Terra, Geofisica, Università di Siena, Via Laterina, 8–53100 *Siena, Italy. E-mail: dario@ibogfs.df.unibo.it*

Accepted 1999 October 1. Received 1999 September 15; in original form 1998 August 21

SUMMARY

Several methods have been proposed to constrain the stress field from fault plane orientations and slip directions within a crustal volume characterized by brittle deformation. All the methods are based on the assumption that the stress field is uniform in the volume considered. If this hypothesis is not checked in advance, however, the methodology may lead to misleading conclusions. In this work, a procedure is defined to check stress-field uniformity by a statistical analysis of the available fault data. Since, in most cases, the statistical features of the uncertainties that affect such data are not well known, a distribution-free approach is proposed. It is based on a simple search algorithm, devoted to selecting stress configurations compatible with available data, combined with a bootstrap resampling approach. The test results are more conservative than the ones so far proposed in the literature. When the test allows stress heterogeneities to be safely excluded, approximate confidence intervals for the principal stress directions can be obtained; otherwise, the level of stress heterogeneity present in the volume under study can be assessed. An application of the proposed procedure to a sample of fault data deduced from seismological data is presented.

Key words: fault plane solutions, inversion, statistical methods, stress distribution.

INTRODUCTION

The definition of the tectonic stress field is of great importance for geodynamic and seismic hazard studies. In situations where direct measurements are lacking, fault data (i.e. fault plane orientations and slip directions) can be used to constrain the regional deviatoric stress field. However, since the unknown mechanical heterogeneities of crustal rocks are the most important factor in controlling fault kinematics, the relationship between the fault geometry and stress responsible for faulting is not unique (McKenzie 1969). Thus, to deduce stress from fault geometries, a number of additional assumptions are necessary (see, e.g. Michael 1984; Gephart and Forsyth 1984; Caputo and Caputo 1988; Angelier 1990; Yin and Ranalli 1993; Choi 1995; Yin 1996).

The first assumption is that, on each fault plane, slip occurs in the direction of the shear stress resolved on the same plane. Furthermore, it is assumed that it is possible to select a crustal volume in which the unknown stress field is uniform. Faults within this volume are thus analysed in order to identify the regional stress field. In particular, the 'best-fitting' stress configuration is sought which minimizes any conventional 'loose' function representative of angular differences between resolved shear stress on the considered fault planes and observed slip. A discussion concerning the statistical and numerical properties of the various 'loose' functions and search procedures so far proposed can be found in Yin and Ranalli (1993).

Despite some reasonable objections (Pollard *et al.* 1993), the assumption that slip direction corresponds to the direction of resolved shear stress on the fault plane seems to be physically plausible and reliable in most cases. On the other hand, as a result of the complexity of tectonic processes, the reliability of the stress uniformity assumption is problematic in many cases. Thus, in order to avoid misleading conclusions, the reliability of this assumption should be carefully checked for each case studied. To this end, two procedures have been proposed, by Wyss *et al.* (1992) and Yin and Ranalli (1993). In both cases, assumptions are required about the statistical properties of the uncertainties that affect observed slip directions and fault orientations: the average values of such uncertainties in the first approach; and the form of the relative parent probability distributions in the second. However, in most cases, the experimental uncertainties that affect individual fault geometries and relative parent distributions are not well known. It is therefore difficult both to make a careful check of stress-field uniformity and to assess reliable confidence intervals for the final results of stress-field inversion. The aim of the present work is to develop a simple algorithm to overcome these difficulties by allowing a check on the stress-field uniformity hypothesis without restrictive assumptions about the experimental uncertainties. In the following, only the principal stress directions will be of concern, and no attempt will be made to obtain information about other important parameters of the stress tensor (e.g. the stress ratio, etc.).

The case of negligible experimental uncertainties is considered first, and a simple distribution-free test is developed on the basis of geometrical and probabilistic considerations. Then, to take experimental errors into account, the test is combined with a numerical resampling procedure which allows the hypothesis of stress-field uniformity to be checked and the confidence intervals for principal stress directions to be approximated.

A DISTRIBUTION-FREE TEST FOR STRESS-FIELD UNIFORMITY

The case of negligible experimental uncertainties

In the assumption of shear faulting, fault geometry is fully described by two perpendicular vectors **U** and **N** (boldface is used in the following to indicate vectors), which represent, respectively, the slip direction and the normal to the fault plane. An alternative description can be supplied by the use of the two axes **T** and **P** related to **U** and **N** by the following vectorial relations:

$$\mathbf{T} = \frac{1}{\sqrt{2}}(\mathbf{U} + \mathbf{N}),$$

$$\mathbf{P} = \frac{1}{\sqrt{2}}(\mathbf{U} - \mathbf{N}) \tag{1}$$

(see, for example, Jost and Herrmann 1989). In practice, the **T** and **P** axes bisect the four solid angles (right dihedra) defined by two perpendicular planes: the 'principal' one, normal to **N**, and the 'auxiliary' one normal to **U**.

The two opposite right dihedra including the **T** axis are said to be dilatational (or T) and the remaining ones are said to be compressional (or P). Eq. (1) shows that interchanging **U** and **N** does not affect the directions of the **T** and **P** axes. This makes the description of fault geometries in terms of the **P** and **T** axes less informative, but particularly useful in the case of seismic fault plane solutions where **U** and **N** cannot be discriminated by seismological data alone. Furthermore, the **T** and **P** directions are physically meaningful, being representative of the principal strain axes ($\boldsymbol{\varepsilon}_3$ and $\boldsymbol{\varepsilon}_1$, respectively) locally accommodated by the fault displacement (Marrett and Allmendinger 1990).

Under the assumption that seismic slip occurs in the direction of the shear stress resolved on the fault plane, it is possible to demonstrate (McKenzie 1969; Carey-Gahilardis and Vergely 1992) that the direction of the principal deviatoric stress $\boldsymbol{\sigma}_1$ responsible for the slip may lie everywhere in the compressional dihedra, while the principal direction $\boldsymbol{\sigma}_3$ is located somewhere in the dilatational dihedra along a direction perpendicular to $\boldsymbol{\sigma}_1$. In particular,

$$\begin{aligned} &|\boldsymbol{\sigma}_1 \cdot \mathrm{T}| > |\boldsymbol{\sigma}_1 \cdot \mathbf{P}|, \\ &|\boldsymbol{\sigma}_3 \cdot \mathrm{T}| < |\boldsymbol{\sigma}_3 \cdot \mathbf{P}|, \\ &\boldsymbol{\sigma}_3 \cdot \boldsymbol{\sigma}_1 = 0, \end{aligned} \tag{2}$$

where the dot indicates the scalar product of the relevant vectors (eigenvalues of the stress tensor are not considered). When relationships (2) hold for a given fault geometry, we can say that this fault geometry is compatible with a stress field represented by the principal stress axes $\boldsymbol{\sigma}_1$ and $\boldsymbol{\sigma}_3$. If all the fault geometries within the volume of interest are compatible with these principal stress directions, they constitute a 'stress-field solution' representative of the actual stress field in the volume under study. This result is the basis of the 'right dihedra' approach proposed by Angelier and Melcher (1977) for the graphical inversion of the stress field from faulting data, and can be used as a simple test for stress-field uniformity: in fact, the lack of a stress-field solution implies that stress is not uniform in the volume under study. However, this condition is necessary but not sufficient for stress-field uniformity. A finite probability exists that, even when the stress field is not uniform, at least one stress field solution will be found by chance. To demonstrate this, we consider the case of N faults within a given crustal volume. In the general case that the stress field is not uniform, the volume can be considered to be composed of K subdomains, each characterized by a uniform stress field significantly different from those active in the other subdomains.

We assume that the stress field active in the ith subdomain is responsible for n_i of the available fault geometries. A tentative direction for the unknown principal stress axis $\boldsymbol{\sigma}_1$ (or $\boldsymbol{\sigma}_3$) is considered. In the case that it corresponds to the actual $\boldsymbol{\sigma}_1$ (or $\boldsymbol{\sigma}_3$) axis in any ith subdomain, the considered direction lies in the P (or T) dihedron corresponding to each of the n_i faults in the ith subdomain. However, since the P (or T) dihedron of each fault includes 50 per cent of all possible directions, a probability of 0.5 exists that, by chance, the explored direction is also compatible with the $N - n_i$ faults that belong to different stress domains. Thus, the probability that all the faults in the crustal volume under study are compatible by chance with the considered direction despite the stress-field inhomogeneity is

$$0.5^{N-n_i}.$$

This probability becomes vanishingly small as N approaches reasonable sample sizes (say, >20). Thus, it appears that an 'apparent' stress-field uniformity can be safely excluded for any practical purpose. However, if the search for possible stress axes is performed by exploring a number M (large) of possible solutions, the probability $P(H_0)$ that at least one direction compatible with the whole set of fault data will be found by chance could become significant. In fact, it holds that

$$P(H_0) = 1 - \prod_{i=1}^{M} (1 - 0.5^{N-n_i}), \tag{3}$$

where n_i is zero when no fault in the sample is the effect of the ith explored principal stress direction, and the number M of explored directions includes both possible $\boldsymbol{\sigma}_1$ and $\boldsymbol{\sigma}_3$ directions. Eq. (3) shows that $P(H_0)$ could become significant for reasonable sample sizes N given that M is sufficiently large.

Various inhomogeneity patterns can be explored with eq. (3). In the extreme case that no explored direction corresponds to any of the active stresses ($n_i = 0$), eq. (3) becomes

$$P(H_0) = 1 - (1 - 0.5^N)^M. \tag{4}$$

If an exhaustive search is performed over a sufficiently dense grid, it seems more realistic to assume that all stress configurations that exist in the K subdomains are actually explored. In this case, eq. (3) assumes the form

$$P(H_0) = 1 - \left[\prod_{i=1}^{K} (1 - 0.5^{N-n_i})\right][(1 - 0.5^N)^{M-K}]. \tag{5}$$

As expected, in the case of a uniform stress field ($K = 1$ in eq. 5), the probability of finding at least one stress-field solution is unity.

The case of the highest level of stress-field complexity that can actually be detected corresponds to the presence of K different subdomains, one for each available fault geometry ($K = N$, $n_i = 1$ and $K < M$). In this case, eq. (5) becomes

$$P(H_0) = 1 - (1 - 0.5^{N-1})^N (1 - 0.5^N)^{M-N}. \quad (6)$$

Some numerical results showing the dependence of $P(H_0)$ on N and M are given in Fig. 1. These results indicate that strong stress-field heterogeneities can be easily detected when a reasonable data set (say, $N > 10$) is available.

This is not true, however, when low levels of heterogeneity in the stress field are of concern. To illustrate this, we note that a low level of stress-field complexity can be associated with the presence of only two stress subdomains in the volume under study. In this case ($K = 2$ in eq. 5), it can be easily shown (Appendix A) that, if there are $N - n$ and n fault geometries in the first and second domain, respectively, when N increases the probability of finding at least one stress-field solution by chance converges to 0.5^n. This result also holds in the case that n stress domains, each responsible for one fault only, coexist in the volume under study with a main stress field responsible for $N - n$ events. How rapidly this convergence occurs as N increases is shown in Fig. 2 for $K = 2$ and $n = 1$, which corresponds to the extreme case of 'least' detectable heterogeneity; that is, the lowest level of stress-field complexity.

These results can be used to check the hypothesis of stress-field uniformity when experimental errors can be considered negligible. The procedure as follows. Taking into account N fault geometries, an exhaustive search is performed over a dense grid of M possible stress directions. If no stress-field solution is found, the hypothesis of stress-field homogeneity can be safely excluded. In the case that at least one solution is found, eqs (3) to (6) can be used to compute the probability that such a solution has been found by chance in the presence of stress heterogeneity: this probability is the significance level corresponding to the hypothesis H_0 that stress field is heterogeneous. As an example, if at least one stress-field solution is found after a grid search carried out over 200 possible directions by taking 20 fault geometries into account, the hypothesis that a high-level stress-field heterogeneity exists in the volume under study (see Fig. 1 and eq. 6) can be safely excluded at a 10^{-3} significance level.

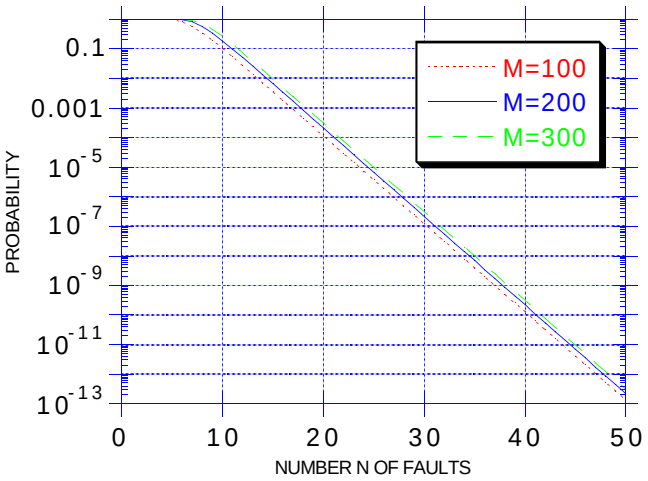

Figure 1. Probability that at least one stress-field solution is found by chance in the presence of the highest possible level of stress heterogeneity. Probability values are given as a function of the number N of available fault geometries and the number M of explored directions for maximum and minimum principal stress. The values have been obtained from eq. (5) with the parameters $K = N$, $n_i = n = 1$.

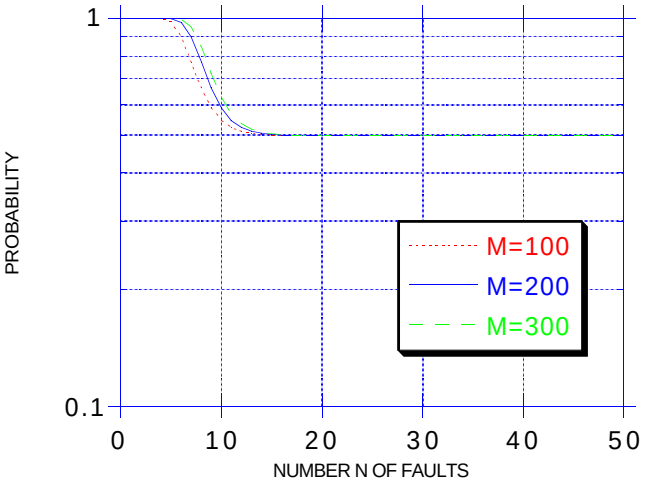

Figure 2. Probability that at least one stress-field solution is found by chance in the presence of the lowest possible level of stress heterogeneity. Probability values are given as a function of the number N of available fault geometries and the number M of explored directions for maximum and minimum principal stress. The values have been obtained from eq. (5) with the parameters $K = 2$, $n_1 = N - 1$, $n_2 = 1$.

General case: taking experimental uncertainties into account

In the previous discussion, the presence of at least one stress-field solution has been considered as a necessary condition for uniformity. On this basis, sufficiency conditions for stress-field uniformity have been analysed by estimating probabilities of 'apparent' uniformity arising by chance for different levels of actual heterogeneity in the stress field. These probabilities do not take into account random fluctuations induced in the data sample by random experimental errors, which result in the apparent 'displacement' of P and T directions from the actual ones. In this situation, it is possible that, by chance, 'apparent' stress homogeneity could arise from a heterogeneous stress field or 'apparent' uniformity could result from a heterogeneous stress field. Thus, the presence of at least one stress-field solution is neither a sufficient nor necessary condition for stress-field uniformity.

As tentatively shown in Appendix B, the case of apparent uniformity induced by experimental errors seems to be less important, at least for a reasonable dimension of the data set, due to its low probability of occurrence. Thus, hereafter we only consider the case of 'apparent' heterogeneity induced by random fluctuations of fault geometrical parameters due to experimental errors. In this case, eqs (3) to (6), being representative of 'true' heterogeneity only, supply upper limits for the probability that at least one stress-field solution is found by chance

under the relevant hypothesis of stress heterogeneity. This reasonable conjecture allows a check to be made of stress-field uniformity when unknown experimental errors are present.

Let us assume that a number L of fault samples are available, each representative of the same active stress field. A grid search of possible stress solutions is performed for each sample, and Q samples characterized by at least one stress-field solution are found. By eqs (3) to (6) the 'upper bound' of probability $P(H_0)$ that at least one stress solution is found by chance is computed under any hypothesis H_0 about the stress-field heterogeneity level. The probability that, by chance, a number Q out of L examined samples are characterized by at least one stress-field solution under any hypothesis (H_0) about the stress-field complexity level is simply found by the binomial equation

$$\sum_{J=Q}^{L} \frac{L!}{J!(L-J)!} P(H_0)[1-P(H_0)]^{L-J}. \quad (7)$$

In the case that such a probability is lower than a threshold α, that specific level of stress-field complexity can be excluded at a significance level α. If this condition is not satisfied, stress-field heterogeneity of the explored type cannot be excluded, no matter whether it is 'true' or 'apparent'.

The test becomes more effective as the sample L becomes larger. Thus, the application of such a procedure to check stress-field uniformity requires a large number of data sets, each resulting from the same stress field and characterized by random experimental variations sampled from the same parent population. Of course, with both the actual stress field and statistical features of the experimental errors being unknown, such data sets cannot be realistically drawn from experimental campaigns. However, as first proposed by Michael (1987) a bootstrap resampling procedure can be used to obtain such data samples from the only available data set.

The bootstrap method (see, e.g. Efron & Tibshirani 1986) is based on the assumption that realizations of a random variable contain all the necessary information about relevant parent probability distribution. This assumption is corroborated by a fundamental result of mathematical statistics which implies that an empirical distribution function is the maximum likelihood estimator of the parent probability distribution of the sampled random variable. It can be shown that, if the experimental data set of n elements is sufficiently extended to be representative of the parent population, each new data sample obtained by randomly extracting (with replacement) n values from the original set is characterized by the same statistical properties as the original sample.

Several numerical procedures can be adopted to obtain such new samples (Efron 1990). The simplest one requires the arrangement of the original data set (of n elements) in the form of a sequential array. Then, a pseudo-random number generator (e.g. Press *et al.* 1992) is used to generate a sequence of n integers in the range from 1 to n. Each number of the random series is used to pick up the corresponding element of the array. The collection of all these elements will represent a 'randomly resampled' data set. This procedure can be iterated in order to obtain an arbitrary number of data sets, each of n elements. In a statistical sense, each new sample is a 'clone' of the original data set. The important point is that such a 'clone' can be realized without any knowledge about parent populations (Efron and Tibshirani 1986).

By using the bootstrap technique, eqs (3) to (7) can be used to check stress-field uniformity in cases in which unknown experimental errors affect the data. The starting set comprises N fault geometries, sampled from a parent multivariate population characterized by unknown statistical properties. By randomly resampling from the original data set, L (a large number) new samples are obtained, each characterized by the same parent population and representative of the same stress field. For each sample, a grid search is performed and the eventual presence of at least one stress-field solution is checked. If Q such cases are actually found, eq. (7) can be used to check the significance level associated with any hypothesis H_0 of stress-field heterogeneity.

Approximate confidence intervals for principal stress directions

The bootstrap procedure described above can also be used to approximate possible confidence intervals for principal stress directions in cases when stress-field heterogeneity can be excluded.

By following the approach described above, L sets, each with N fault geometries, are obtained by randomly resampling (with replacement) from the original data set, also comprising N fault plane solutions. For each set, M possible directions are evaluated as possible principal stress directions compatible with the relevant set of resampled fault plane solutions. Out of the L runs, the mth direction resulted in a possible principal stress direction $r(m)$ times. If L is large, the ratio $r(m)/L$ can be considered an estimate of the probability P that the direction m actually represents a principal stress direction compatible with the original data set.

Thus, the set of those directions m such that

$$r(m)/L > \alpha \quad (8)$$

approximates the $1-\alpha$ confidence interval for the inferred principal stress axis.

Confidence intervals defined in this way include a number of possible stress-field solutions, each characterized by the same reliability. Since no 'best fit' criterion has been introduced, it is not possible to select any particular solution as the 'best' one.

A CASE STUDY

The approach described above to check stress-field uniformity and to approximate confidence intervals for inverted principal stress directions has been applied to the data set reported in Table 1 for the hypothesis that unknown experimental errors affect the data. This sample comprises 25 seismic fault plane solutions analysed by Cocina *et al.* (1997) to constrain the stress-field in the western sector of the Etna Volcano (southern Italy) at crustal depths ($h \geq 10$ km). By following the approach proposed by Gephart and Forsyth (1984) and Wyss *et al.* (1992), which is a standard procedure for stress-field inversion (see also Caccamo *et al.* 1996; Frepoli & Amato 1997; Eva *et al.* 1997), Cocina *et al.* (1997) suggest that the stress field in the explored crustal volume is uniform. In order to check this conclusion, the data set in Table 1 has been analysed using the bootstrap procedure proposed here.

Up to 10^4 samples have been generated by randomly resampling from the data set in the Table. For each sample, a grid of 253 possible directions for principal stress axes has

Table 1. Earthquake fault plane solutions used by Cocina *et al.* (1997) to constrain the stress field in the western sector of the Etna Volcano (southern Italy). Fault geometries are indicated by T and P directions, each represented in terms of trend (degrees eastwards) and plunge (degrees from the horizontal). Mag is the earthquake magnitude.

N	Year	Mon	Day	H	Min	Lat. (°N)	Lon. (°E)	Mag	Depth km	P axis		T axis	
										tr. (°)	pl. (°)	tr. (°)	pl. (°)
1	1990	9	3	6	36	37.76	14.96	1.5	26	213	24	9	63
2	1990	9	3	9	43	37.77	14.95	1.6	24	220	22	358	60
3	1990	9	3	10	52	37.76	14.95	1.5	28	220	22	358	60
4	1991	1	26	10	36	37.7	14.98	1.5	31	265	10	360	24
5	1991	1	26	13	12	37.71	14.97	1.1	25	65	77	203	9
6	1991	1	27	4	46	37.71	14.98	1.1	24	72	52	177	11
7	1991	1	27	11	12	37.71	14.98	1.1	26	169	80	350	10
8	1991	1	27	15	36	37.71	14.98	1.2	22	270	14	173	27
9	1991	1	27	18	38	37.72	14.98	1.1	22	310	72	194	8
10	1991	4	20	15	48	37.75	14.97	1.8	22	223	24	19	63
11	1991	4	20	15	51	37.76	14.95	1.5	27	242	17	338	17
12	1991	4	20	16	0	37.75	14.95	1.6	22	237	2	331	58
13	1991	4	20	16	1	37.74	14.95	1.6	21	47	3	314	31
14	1991	4	20	21	24	37.76	14.94	1.4	23	240	6	334	21
15	1991	4	20	21	28	37.76	14.96	1.3	21	245	10	340	24
16	1991	4	21	1	42	37.76	14.98	1.9	26	50	3	319	17
17	1991	4	21	1	51	37.77	14.94	1.8	23	227	3	319	25
18	1991	4	21	3	12	37.76	14.94	1.6	25	237	3	329	25
19	1991	5	15	17	19	37.75	14.97	1.9	27	57	2	324	60
20	1991	5	15	17	57	37.76	14.94	1.2	20	71	13	339	13
21	1991	5	15	18	42	37.74	14.95	1.5	19	238	5	332	35
22	1991	7	13	15	30	37.73	14.99	1.0	26	36	25	128	3
23	1991	7	16	13	20	37.74	14.98	2.8	27	67	6	331	45
24	1991	7	16	15	39	37.75	14.97	2.7	28	63	6	327	44
25	1991	9	24	0	4	37.68	14.97	1.5	28	294	38	203	1

been explored. These directions have been selected by following the procedure in Appendix C in order to ensure a uniform coverage of the equi-area stereonet with an average density of about 5°. For each run, the presence of at least one 'stress-field solution' (see eq. 2) has been checked. The relative frequency of such cases as a function of the number of samples considered is reported in Fig. 3 (pattern A). This frequency tends to stabilize around a value of 0.26 (2632 out of 10^4 trials) after a few thousand iterations.

By using eqs (6) and (7) with $N = 25$, $M = 253$, $L = 10^4$ and $Q = 2632$, the hypothesis of maximum heterogeneity can be excluded at a high confidence level ($P < 10^{-6}$). However, a low level of heterogeneity cannot be excluded with the same high confidence level. This can be seen by assuming that only two stress subdomains exist, and that one of them is responsible for one fault geometry only (least-stress heterogeneity). In this case, eqs (5) and (7) (with $N = 25$, $M = 253$, $K = 2$, $n = 1$, $L = 10^4$ and $Q = 2632$) indicate a probability $P(H_0)$ near unity. This result implies that stress-field heterogeneity of the lowest level cannot be excluded. Further applications of eqs (5) and (7) allow intermediate levels of stress heterogeneity to be excluded in the crustal volume under study.

In the hypothesis that stress heterogeneity is not an artefact resulting from wrong data, a different data selection can be performed in order to identify the subvolumes characterized by a 'uniform' stress field. Such a subvolume could be the one below 11 km depth. In this case, the bootstrap procedure

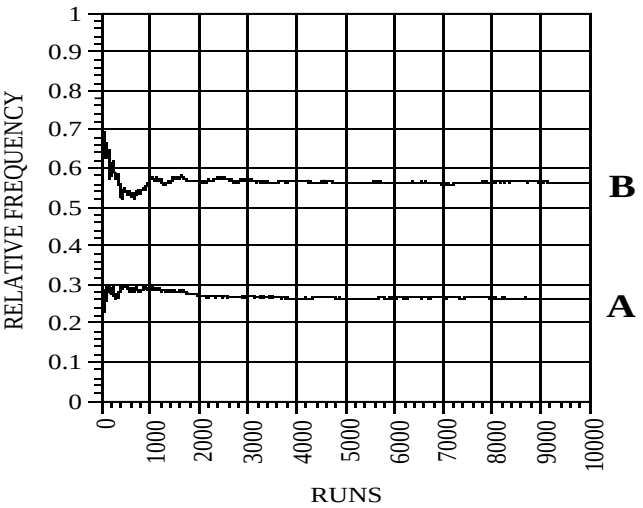

Figure 3. Results of the test for stress-field uniformity performed using the data in Table 1. In the plot, the relative frequency of bootstrap iterations that allowed at least one stress solution compatible with the relevant resampled data set to be found is reported as a function of the number of bootstrap runs. (A) Results obtained using the data set in Table 1; (B) results obtained using the same data set with the exclusion of the event that occurred on 1991/7/13. For each bootstrap iteration, 253 directions were explored with an average grid density of about 5°.

(pattern B in Fig. 3) suggests a relative frequency of samples characterized by at least one stress solution higher than 0.5. By using eqs (5) and (7), it can be easily shown that, in this case, stress-field heterogeneity can be safely excluded also in the case of the lowest level of stress-field complexity.

Since the stress field can be now assumed to be uniform, the bootstrap procedure can be used (eq. 8) to approximate 95 per cent confidence intervals for principal stress directions. Results of this analysis after 10^4 bootstrap trials are given in Fig. 4. Confidence intervals appear to be larger than the ones obtained by Cocina *et al.* (1997) (Fig. 4), and include the 'best-fitting' solutions obtained by these authors.

CONCLUSIONS

A distribution-free approach for testing stress-field uniformity with regard to fault geometry (plane orientation and slip direction) has been proposed. The test is based on a numerical resampling procedure (bootstrap), which is computationally simple and can easily be implemented in an efficient computer code. Since only fault geometries are considered, the test can be used for both structural and seismic data.

The basic assumption underlying the proposed approach is that fault slip occurs in the direction of shear stress resolved on the fault plane. No detailed knowledge of the uncertainties that affect fault geometries is required, but the data set must be known to be representative of the unknown parent population. All other assumptions, both concerning conventional 'best-fitting' criteria or statistical properties of parent populations of fault parameters, are unnecessary.

The test proposed here tends to be more conservative than other parametric tests (see, for example, Yin & Ranalli 1993), since it assumes stress heterogeneity as the hypothesis to be rejected by testing data: in practice, the stress field is supposed to be heterogeneous and data are used to falsify this hypothesis. This position seems to be more in line with geological information, which suggests strong variations in the crustal stress field as a result of strength heterogeneities at several scales (see, for example, Rebai *et al.* 1992). Thus, in cases in which insufficient information is available, stress heterogeneity is not excluded *a priori*, and possible misleading conclusions resulting by faulty assumptions of stress uniformity are avoided.

Another advantage of the test described here is that several levels of stress-field heterogeneities can be explored and, possibly, rejected. This could provide useful information about local stress-field features and drive the search for uniform-stress crustal subvolumes.

The approach does not allow an 'optimal' stress-field solution to be found from the available data. This is the result of the choice not to take into account conventional 'best-fit' criteria. It is not a limitation of the proposed procedure, which aims to check stress-field uniformity only: other more efficient and complete approaches (e.g. Yin & Ranalli 1993) can be used to assess best-fitting solutions and stress ratios when stress uniformity has been safely assessed. Furthermore, since approximate confidence intervals for the principal stress directions can be obtained by the present approach, these can be used to select the initial positions required for non-linear inversion procedures (for example Gephart & Forsyth 1984).

An application of the present approach to real data has been given. It has been shown that, at least in the case considered here, this approach is more sensitive than the one proposed by Wyss *et al.* (1992) for detecting stress-field heterogeneities. Furthermore, it has been shown how the present approach allows the level of stress complexity in the volume under study to be determined, and how this information can be used to identify uniform-stress subvolumes. A comparison

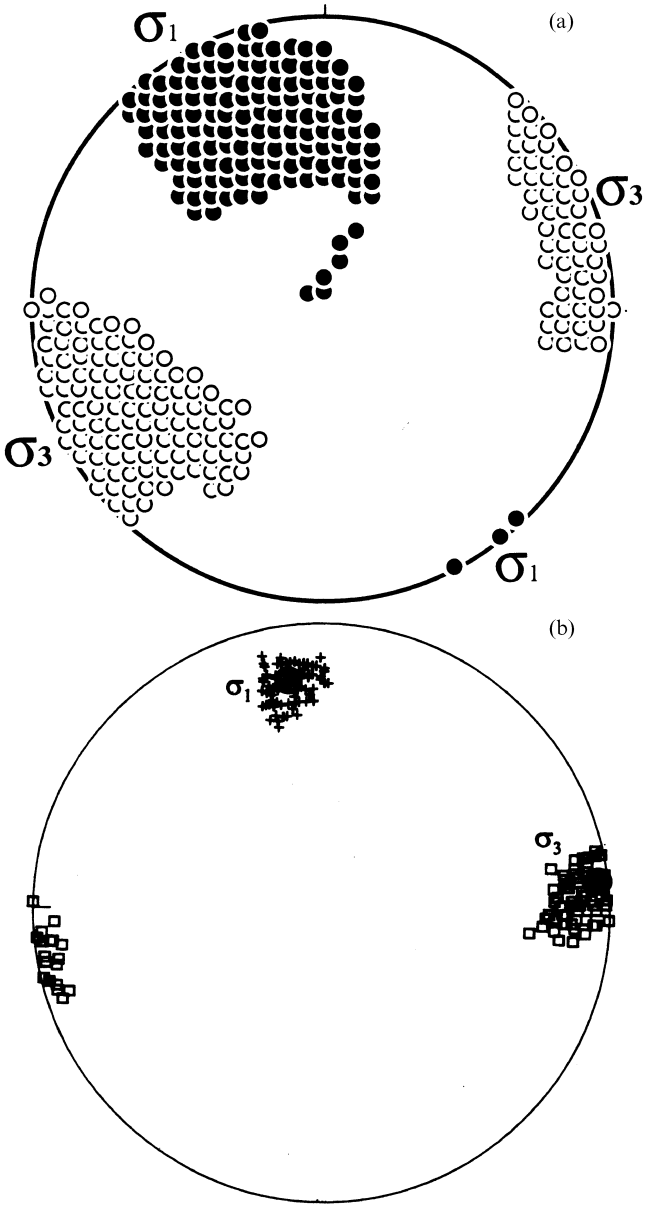

Figure 4. Comparison of confidence intervals for the maximum and minimum principal stress directions obtained using the bootstrap approach proposed here (a) and those obtained by Cocina *et al.* (1997) (b). (a) Dark and white circles in the stereonet indicate approximate 95 per cent confidence intervals for σ_3 and σ_1, respectively, after 10^4 bootstrap iterations, using for each iteration a grid search performed over 253 directions (which corresponds to an average grid density of about 5°), and the data shown in Table 1, with the exception of the event that occurred on 1991/7/13. (b) Crosses and small squares, respectively, indicate 95 per cent confidence intervals for σ_3 and σ_1 proposed by Cocina *et al.* (1997). Circles indicate the positions of the 'best-fitting' directions of the principal stress axes (after Cocina *et al.* 1997). An equal area lower emisphere projection is used. North is upwards and east is to the right.

of approximate confidence intervals for principal stress axes obtained by the proposed procedure with those obtained by a 'standard' methodology suggests that the latter, at least for the case considered here, tends to seriously underestimate the actual uncertainty of the principal stress directions.

ACKNOWLEDGMENTS

I am indebted to Prof. G. Ranalli for his careful reading of the manuscript, fruitful suggestions and stimulating comments which clarified the presentation and my thinking on the questions raised in this paper. Support for this work has been provided by Gruppo Nazionale di Geofisica della Terra Solida and Ministero dell'Università e della Ricerca Scientifica.

REFERENCES

Aki, K. & Richards, P.G., 1980. *Quantitative Seismology, Theory and Methods,* Freeman & Co., New York.

Angelier, J., 1990. Inversion of field data in fault tectonics to obtain the regional stress, III. A new rapid direct inversion method by analytical means, *Geophys. J. Int.,* **103,** 363–376.

Angelier, J. & Melcher, P., 1977. Sur une methode graphique de recherche des contraintes principales egalment utilisable en tectonique et en seismologie: methode des diedres droits, *Bull. Soc. geol. France,* V, **19,** 1309–1318.

Caccamo, D., Neri, G., Sarao, A. & Wyss, M., 1996. Estimates of stress directions by inversion of earthquake fault plane solutions in Sicily, *Geophys. J. Int.,* **125,** 857–868.

Caputo, M. & Caputo, R., 1988. Structural analysis: new analytical approach and applications, *Ann. Tecton.,* **2,** 84–89.

Carey-Gahilardis, E. & Vergely, P., 1992. Graphical analysis of fault kinematics and focal mechanisms of earthquakes in terms of stress: the right dihedra method, use and pitfalls, *Ann. Tecton.,* **6,** 3–9.

Choi, P.-Y., 1995. Aspects of stress inversion methods in fault tectonic analysis, *Ann. Tecton.,* **9,** 22–38.

Cocina, O., Neri, G., Privitera, E. & Spampinato, S., 1997. Stress tensor computations in the Mount Etna area (southern Italy) and tectonic implications, *J. Geodyn.,* **23,** 109–127.

Efron, B., 1990. More efficient bootstrap computations, *J. Am. stat. Ass.,* **85,** 79–89.

Efron, B. & Tibshirani, R., 1986. Bootstrap methods for standard errors, confidence interval and other measures of statistical accuracy, *Stat. Sci.,* **1,** 54–77.

Eva, E., Solarino, S., Eva, C. & Neri, G., 1997. Stress tensor orientations derived from fault plane solutions in the Southwestern Alps, *J. geophys. Res.,* **102,** 8171–8185.

Frepoli, A. & Amato, A., 1997. Contemporaneous extension and compression in the Northern Apennines from earthquake fault plane solutions, *Geophys. J. Int.,* **129,** 368–388.

Gephart, J.V. & Forsyth, D.W., 1984. An improved method for determining the regional stress tensor using focal mechanisms data: application to the S. Fernando earthquake sequence, *J. geophys. Res.,* **89,** 9305–9320.

Jost, M.L. & Herrmann, R.B., 1989. A student's guide to and review of moment tensors, *Seism. Res. Lett.,* **60,** 37–57.

McKenzie, D.P., 1969. The relation between fault plane solutions for earthquakes and the directions of the principal stresses, *Bull. seism. Soc. Am.,* **59,** 591–601.

Marrett, R. & Allmendinger, R.W., 1990. Kinematic analysis of fault slip data, *J. struct. Geol.,* **12,** 973–986.

Michael, A.J., 1984. Determination of stress from slip data: faults and folds, *J. geophys. Res.,* **89,** 11 517–11 529.

Michael, A.J., 1987. Use of focal mechanisms to determine stress: a control study, *J. geophys. Res.,* **92,** 357–368.

Pollard, D.D., Salzer, S.D. & Rubin, A.M., 1993. Stress inversion methods: are they based on faulty assumptions? *J. struct. Geol.,* **15,** 1045–1054.

Press, W.H., Teukolsky, S.A., Vetterling, W.T. & Flannery, B.P., 1992. *Numerical Recipes,* 2nd edn, Cambridge University Press, Cambridge.

Rebai, S., Philip, H. & Taboada, A., 1992. Modern tectonic stress filed in the Mediterranean region: evidence for variations in stress directions at different scales, *Geophys. J. Int.,* **110,** 106–141.

Wyss, M., Liang, B., Tanigawa, W.R. & Wu, X., 1992. Comparison of orientation of stress and strain tensors based on fault plane solutions in Kaoiki, Hawaii, *J. geophys. Res.,* **97,** 4769–4790.

Yin, Z.-M., 1996. An improved method for the determination of tectonic stress field from focal mechanism data, *Geophys. J. Int.,* **125,** 841–849.

Yin, Z.-M. & Ranalli, G., 1993. Determination of tectonic stress field from fault slip data: towards a probabilistic model, *J. geophys. Res.,* **98,** 12 165–12 176.

APPENDIX A: $P(H_0)$ FOR LOW LEVELS OF STRESS-FIELD METEROGENEITY IN THE LIMIT OF N LARGE

In the case that $K = 2$, $n_1 = N - n$ and $n_2 = n$, eq. (5) becomes

$$P(H_0) = 1 - [(1 - 0.5^n)(1 - 0.5^{N-n})][(1 - 0.5^N)^{qN-2}], \quad \text{(A1)}$$

where $M = qN$ with $q > 1$. When N increases, $N \gg n$, and thus $N - n \cong N$, which implies

$$P(H_0) \cong 1 - [1 - 0.5^n][(1 - 0.5^N)^{qN-1}]. \quad \text{(A2)}$$

Furthermore, since

$$(1 - 0.5^N)^{qN-1} = \exp[(qN - 1)\ln(1 - 0.5^N)], \quad \text{(A3)}$$

by a first-order McLaurin approximation we obtain that

$$(1 - 0.5^N)^{qN-1} \cong \exp[-(qN - 1)/2^N], \quad \text{(A4)}$$

which rapidly converges to 1 as N increases. This implies that

$$P(H_0) \cong 0.5^n. \quad \text{(A5)}$$

In the case that $K = n + 1$, $n_1 = N - n$ and $n_i = 1$ (varying i from 2 to $n + 1$), eq. (6) becomes

$$P(H_0) = 1 - [(1 - 0.5^n)(1 - 0.5^{N-1})^n][(1 - 0.5^N)^{qN-n-1}], \quad \text{(A6)}$$

by the substitution of M with qN (with $q > 1$).

Moreover, when N increases, $N - 1 \cong N$, and thus

$$P(H_0) = 1 - [1 - 0.5^n][(1 - 0.5^N)^{qN-1}], \quad \text{(A7)}$$

which again implies for increasing N that

$$P(H_0) \cong 0.5^n. \quad \text{(A8)}$$

APPENDIX B: PROBABILITY THAT APPARENT STRESS-FIELD HOMOGENEITY MAY ARISE BY CHANGE

A finite probability exists that random experimental errors can result, by chance, in 'apparent' uniformity of the stress field. One can suppose that the effect of random errors is to 'displace' the actual direction of a P (or T) axis towards a new 'apparent' position. Apparent uniformity arises when all the 'displaced' directions fall in the same dihedron. In the absence of systematic errors, the probability that this occurs by chance for N fault plane solutions is of the order of 0.5^N. In the case

that M possible dihedra are explored, the probability that, due to random fluctuations, at least one of them can collect all P (or T) axes can be estimated by

$$1-(1-0.5^N)^M, \tag{B1}$$

which becomes rapidly small as N increases. As an example, for $M=200$ and $N=15$, the probability that 'apparent' uniformity is induced by random errors is 0.6 per cent.

APPENDIX C: GRID FOR THE SEARCH OF POSSIBLE STRESS-FIELD SOLUTIONS

It is clear that a grid search performed over the lower hemisphere, allowing the trend (ϕ) and plunge (λ) angles to vary in the intervals

$$\phi \in [-\pi, +\pi],$$

$$1 \in [0, \pi/2] \tag{C1}$$

with a uniform angular step δ for both ϕ and λ does not result in a uniform grid. In fact, the grid elements tend to concentrate around the direction normal to the horizontal plane. In order to obtain an effective search for stress direction, the areal density of grid elements should be uniform. To this end, the grid has been defined over the equi-area stereonet projection (Wulff net) of the hemisphere. A unitary Wulff stereonet can be obtained by using the relationships

$$x_i = \sin[(\pi/4)-(\lambda_i/2)]\cos(\phi_i),$$

$$y_i = \sin[(\pi/4)-(\lambda_i/2)]\sin(\phi_i) \tag{C2}$$

(see, for example, Aki & Richards 1980) which reproduces the hemisphere on a plane circular surface of unitary radius: values x_i and y_i represent coordinates on the plane corresponding to the ith direction defined by the couple (ϕ_i, λ_i). A uniform coverage of the hemisphere can thus be obtained if x and y are allowed to vary in the intervals

$$x_i \in [-1, +1],$$

$$y_i \in [-1, +1],$$

$$(x_i^2 + y_i^2)^{1/2} \leq 1 \tag{C3}$$

with uniform step Δ along both the x and y axes. Directions for the grid search can be easily obtained by converting these positions in space directions using the inverse of eqs (C2), which is given by

$$\phi_i = \tan^{-1}(x_i/y_i),$$

$$\lambda_i = \pi/2 - 2\sin^{-1}[y_i/\cos(\phi_i)]. \tag{C4}$$